Rate Constant for the Reaction of Cl_2(aq) with OH^-

M. Gershenzon and P. Davidovits*

Department of Chemistry, Merkert Chemistry Center, Boston College, Chestnut Hill, Massachusetts 02467-3809

J. T. Jayne, C. E. Kolb, and D. R. Worsnop

Center for Aerosol and Cloud Chemistry, Aerodyne Research Inc., Billerica, Massachusetts 01821-3976

Received: November 12, 2001; In Final Form: June 17, 2002

The second-order rate constant (k_2) for the aqueous-phase reaction $Cl_2(aq) + OH^- \rightarrow HOCl + Cl^-$ was determined by measuring the uptake of gas-phase chlorine into water in a bubble train flow reactor. In making these measurements, we avoided some of the difficulties encountered in earlier studies. Data were obtained at 275, 293, and 303 K, yielding $k_2 = (1.3 \pm 0.5) \times 10^8$ M^{-1} s^{-1}, $(6 \pm 2) \times 10^8$ M^{-1} s^{-1}, and $(8 \pm 3) \times 10^8$ M^{-1} s^{-1}, respectively. The atmospheric relevance of the chlorine hydrolysis reaction is discussed.

Introduction

Global average concentrations of chlorine in the troposphere are as high as 10^4 cm^{-3}.[1,2] However, elevated levels of molecular chlorine ($\sim 10^9$ cm^{-3}) in the nighttime marine boundary layer were recently measured in the coastal air of Long Island.[3] This measurement, combined with earlier deductions about atmospheric reactive chlorine concentrations,[4−6] has motivated studies examining possible mechanisms for the release of photolabile chlorine species from sea-salt aerosol particles. The most likely pathways for conversion of sea-salt chloride to aqueous molecular chlorine involve heterogeneous reactions where the initial step is the reaction of Cl^- with one or more of the atmospheric trace gases OH, NO_3, O_3, and $ClNO_3$.[4,7−10] Once generated within the aerosol, chlorine may diffuse out of the particle into the gas phase or it may react within the particle and be retained as an aerosol species. The fraction of chlorine volatilized to the gas phase is determined by competition between the rates of chemical sinks for Cl_2(aq) and the diffusion rate of the species out of the particle.

Chlorine hydrolysis is one possible pathway for the conversion of aqueous chlorine to an aerosol reservoir species. That is,

$$Cl_2(aq) + H_2O \overset{k_1}{\rightleftharpoons} HOCl + H^+ + Cl^- \qquad (R1)$$

$$Cl_2(aq) + OH^- \overset{k_2}{\rightleftharpoons} HOCl + Cl^- \qquad (R2)$$

Reaction rates for the formation and consumption of aqueous chlorine are required to model the production rate of gas-phase chlorine. For example, in recent smog chamber experiments in which Cl_2(g) production from aqueous salt aerosols was studied, Knipping et al. demonstrated[10,11] that as the aerosol pH increased to 10.8 the Cl_2(aq)/OH^- reaction dominated the consumption of chlorine.

Rates for reaction R1 as well as the equilibrium constant for the overall process R1 + R2 are well established.[12] However, literature values for the rate constant k_2 (the forward reaction of R2) span 4 orders of magnitude.

Whereas the current interest in these reactions is motivated by their possible role in atmospheric chemistry, reactions R1 and R2 are central to several other important processes, among which is the formation of the industrial bleaching agent hypochlorite and the disinfecting of water by chlorination. Thus, the study of reactions R1 and R2 has a long history, which is discussed by Knipping and Dabdub.[11] Here, we will provide a summary and brief evaluation of the literature data for the $Cl_2(aq) + OH^-$ second-order rate constant k_2.

The first chlorine hydrolysis studies were published in 1936 by Shilov and Solodushenkov.[13] A subsequent 1945 article by the same authors[14] states that the original results were in error; therefore, the value for k_2, calculated by Morris,[15] that is based on these results is invalid. An upper limit of k_2 published in 1956 by Anbar and Taube[16] is likewise not useful because at 8.3×10^{12} M^{-1} s^{-1} this upper limit exceeds the diffusion-controlled rate by almost 3 orders of magnitude. Subsequently published values for k_2 with references are listed in Table 1. The Table also provides brief summaries of the methods used to obtain k_2 values.

As is evident, the k_2 values listed in Table 1 differ by 4 orders of magnitude. The uncertainties inherent in these studies can be understood in terms of the experimental techniques used. As indicated in the Table, these techniques can be classified into two broad categories: homogeneous and heterogeneous. In the homogeneous studies, chlorine is predissolved in water, and then chemical equilibrium is perturbed either by a step dilution of the solution with water[12,17] or by a temperature jump.[18] The value of k_2 is obtained from the rate of return to equilibrium. In the heterogeneous studies, gas-phase chlorine is brought into contact with the aqueous solution containing OH^-. Here, k_2 is obtained either from the rate of appearance of aqueous species Cl_2(aq) or Cl^- [19,20] or from the rate of disappearance of Cl_2(g) as it is taken up by the solution.[21]

In the homogeneous studies listed in Table 1, the Cl_2(aq)/OH^- reaction rate is too rapid to have been measured directly. The values of Lifshitz and Perlmutter-Hayman[17] as well as those of Wang and Margerum[12] are estimates that are based on indirect measurements. These groups studied much slower but mechanistically similar reactions of Cl_2(aq) with CH_2ClCOO^-, $HCOO^-$, SO_4^{2-}, and $H_2PO_4^-$ and then applied an empirical

* Corresponding author. E-mail: paul.davidovits@bc.edu.

10.1021/jp014146b CCC: $22.00
Published on Web 08/02/2002

TABLE 1: Summary of the $Cl_2(aq)/OH^-$ Rate Constant Measurements[a]

reference	k_2, $M^{-1} s^{-1}$	comment
17	1×10^9 (estimated) at $T = 282.7$ K	Homogeneous study with k_2 estimated via extrapolation of Bronsted−Pedersen equation of the relatively slow reaction rates of $Cl_2(aq)$ with CH_2ClCOO^- and $HCOO^-$. Experimental condition: pH = 2
18	1×10^{10} (estimated) at $T = 303$ K	Homogeneous study with k_2 estimated from the rate of return to equilibrium after temperature jump. Here, reaction R1 dominates, and k_2 is only an estimate. Experimental conditions: pH = 1−2
19	1×10^6 (estimated) at $T = 298$ K	Heterogeneous study with k_2 estimated from $Cl_2(g)$ absorption rate in a laminar liquid jet reactor with $Cl_2(aq)$ iodometric detection. Experimental conditions: pH = 14.1, 14.2
21	2.7×10^7 at $T = 273$ K	Heterogeneous study with k_2 deduced from $Cl_2(g)$ absorption rate in a roller-drum reactor with $Cl_2(g)$ detection. Experimental conditions: $[OH^-] = (2-14)$ M
12	1×10^{10} (estimated) at $T = 288$ K	Homogeneous study with k_2 estimated via extrapolation of Bronsted−Pedersen equation of the relatively slow reaction rates of $Cl_2(aq)$ with CH_2ClCOO^- and $HCOO^-$ (ref 17), SO_4^{2-}, and $H_2PO_4^-$. Experimental condition: pH = 1
20	1.7×10^9 at $T = 293$ K 1.2×10^9 at $T = 298$ K 1.8×10^9 at $T = 303$ K 2.1×10^9 at $T = 312$ K (estimated)	Heterogeneous study with k_2 estimated from $Cl_2(g)$ uptake in a laminar liquid jet absorber with $Cl^-(aq)$ detection. Experimental conditions: $T = (293-312)$ K, pH = 13

[a] Chronological order.

Bronsted−Pedersen relationship to extract the $Cl_2(aq)/OH^-$ rate constant. Aside from the question of the applicability of the Bronsted−Pedersen law to the H_3O^+/H_2O and OH^-/H_2O systems discussed by Knipping and Dabdub [11], there is the issue of the uncertainty introduced by extrapolation to values that are 5 orders of magnitude higher than the experimental data.

To slow the $Cl_2(aq)$ hydrolysis, the homogeneous studies of Eigen and Kustin[18] were performed in a regime (pH = 1−2) where reaction R1 dominates the kinetics. In this region, the $Cl_{2(aq)}/OH^-$ reaction has only a small effect, and k_2 could only be estimated.

In general, the accuracy of the k_2 determination obtained via heterogeneous experiments was limited by the low detection sensitivities available in those studies. To detect the reactants/products, high species concentrations had to be used. The experiments of Spalding[19] and Ashour et al.[20] were performed at high $Cl_2(g)$ concentrations ($[Cl_2(g)] = 1$ atm in both studies), thus depleting the near-surface concentration of OH^- very quickly, and the $Cl_2(g)$ uptake rate was mainly determined by the slow liquid-phase diffusion of OH^- and $Cl_2(aq)$. Accordingly, as stated by the authors, their values of k_2 are estimates.

In the absorption studies of Sandall et al.,[21] the $Cl_2(g)$ density was lower than in the experiments of Spalding[19] and Ashour et al.,[20] although it was still relatively high, in the range of 1 to 3 Torr. The main source of uncertainty in these experiments was the high OH^- concentration. The Sandall et al. experiments[21] were designed to be first order in OH^-. Accordingly the OH^- concentration in the solution was in the range 2−14 M. Here the rate constant k_2 was obtained by extrapolating experimental data to the region of low OH^- concentration. However, at high OH^- concentrations, both the rate constant and the diffusion coefficient required to calculate it may be significantly different from values at low OH^- concentrations. The long-range extrapolation is likely to be a source of error in their quoted value of k_2.

Faced with the uncertainty in k_2 literature values, as evident in Table 1, Knipping and Dabdub chose the value of $k_2 = 1 \times 10^8$ M^{-1} s^{-1} to analyze their aerosol chamber data.[11] This number is close to the logarithmic average of the tabulated k_2 values.

In addition to the studies listed in Table 1, several heterogeneous experiments were done under conditions where the concentrations of gas-phase and solvated chlorine were much greater than the concentration of OH^- in the liquid phase.[22,23] In such experiments, the near-surface OH^- is very quickly depleted, and the rate of $Cl_2(g)$ disappearance is governed by the liquid-phase diffusion rate to the reaction plane rather than k_2.

In the work presented here, we report values of k_2 for the $Cl_2(aq)/OH^-$ reaction obtained via $Cl_2(g)$ uptake measurements. Because of improved detection sensitivity, the experiments were conducted at relatively low reagent concentrations ($Cl_2(g)$ number density near 10^{14} cm^{-3} (3×10^{-3} Torr) and OH^- concentration in the range 1×10^{-6} to 1×10^{-3} M), thus circumventing many of the difficulties encountered in the earlier studies.

Experimental Method

The operation of the horizontal bubble train apparatus has been described in detail.[24−26] Here we provide a brief description of the method and describe the modified detection system.

Water containing a known concentration of OH^- is pumped through a 0.4-cm i.d. quartz tube at a controlled speed of about 20−25 cm s^{-1}. A low-pressure (100 Torr) He gas flow containing $Cl_2(g)$ at a number density of $\sim 10^{14}$ cm^{-3} is injected into the liquid flow via 1.6-mm stainless steel tubing. Upon injection, the gas forms well-defined bubbles. An experimental run begins with the injector positioned outside the flow tube with the gas flowing through the injector without contacting the liquid, producing a "noncontact" signal, which is recorded. The computer-controlled translation stage then starts to draw the injector into the flow tube filled with the flowing liquid. Well-defined bubbles, approximately 0.6 cm long and 0.4 cm in diameter (filling the diameter of the tube), are formed as the injector enters the liquid. The surface area of the bubble, including the effect of bubble shape as discussed in ref 24, is ~ 1 cm^2, and bubble volume is ~ 0.1 cm^3. The size, speed, and frequency of the bubbles are monitored by light-emitting diodes positioned 20 cm from the exit of the flow tube. The liquid flow carries the bubbles to the end of the flow tube where the bubbles open and release the entrained gas, which is continuously detected by a mass spectrometer. The position of the injector within the flow tube where a given bubble is generated and the speed of the bubbles determine the $Cl_2(g)$−liquid interaction time. The depletion of $Cl_2(g)$ as a function of the gas−liquid interaction time is used to calculate k_2 for the $Cl_2(aq)/OH^-$ reaction.

In these experiments, the use of chemical ionization mass spectrometry (CIMS) significantly improved $Cl_2(g)$ detection sensitivity compared to that of previously used electron impact ionization mass spectrometry. Here, $Cl_2(g)$ is ionized in a separate gas flow tube via charge exchange with SF_6^- ions. The SF_6^- ions are produced by passing the SF_6/N_2 mixture over a radioactive ^{210}Po source. The ions are then mixed with the $Cl_2(g)$-containing gas flow from the bubble train flow tube. The resulting $Cl_2^-(g)$ ions are then extracted into the quadrupole mass spectrometer with electrostatic lenses. This implementation of $Cl_2(g)$ chemi-ionization improves detection sensitivity by about 2 orders of magnitude.

The gas flow exiting the bubble train flow tube contains water vapor at 100% relative humidity. At such a high water vapor concentration, water molecules tend to cluster around negative ions, resulting in a more complex mass spectrum. To reduce the formation of water clusters, dry nitrogen is introduced into the region of ion extraction. In this low water-vapor environment, the clusters break up. With this technique, the cluster density is decreased by about 90%, and the sensitivity of the detection scheme is enhanced by approximately a factor of 2.

The $Cl_2(g)$/He mixture was prepared by diluting chlorine with helium at a $Cl_2(g)$/He ratio in the range of $(0.5-5) \times 10^{-4}$. The mixture was stored in a Teflon-coated stainless steel cylinder. Helium and $Cl_2(g)$ were obtained from AGA Gas Inc. (99.999% purity). Solution pH was set by adding NaOH and HCl (Aldrich Chemical Co., Inc., certified A.C.S. Plus grade purity). No pH buffers were used. To remove trace amounts of Br^- ions in the hydrochloric acid, ozone was bubbled through the acid solution for 2 h prior to the experiment. All other chemicals were used without further purification. Millipore Milli-Q filtered water (resistivity > 18 MΩ cm at 25 °C) was used in all of the studies.

Modeling Chlorine Uptake

In the absence of chemical reactions, gas uptake by a liquid is governed by gas-phase diffusion, mass accommodation, and by solubility constraints as the species in the liquid approach Henry's law saturation. In this case, the flux of the gas-phase species diminishes with time, and the total amount of gas absorbed during a time period t per cm^2 into a semi-infinite nonreactive liquid can be expressed as[27]

$$\int_0^t J(t')\,dt' = 2n_g HRT\sqrt{\frac{D_l t}{\pi}} \tag{1}$$

Here, J is the flux of molecules from the gas phase to the liquid surface, n_g is the density of the trace gas, R is the gas constant (0.082 dm^3 atm K^{-1} mol^{-1}), D_l (cm^2 s^{-1}) is the liquid-phase diffusion coefficient of the trace species, H (M atm^{-1}) is the Henry's law coefficient, T(K) is the temperature, and t' is the variable of integration.

Chemical reactions of the solvated species in the bulk liquid or at the gas/liquid interface provide a sink for the species, thus counteracting the effect of saturation. The enhancement of gas uptake due to chemical reactions of the solvated species in the bulk liquid can be expressed in terms of an enhancement factor E as defined by Dankwerts.[27] This factor is the ratio of the amount of gas absorbed during time t in a chemically enhanced process to the amount of gas that would have been absorbed during the same period due to uptake governed by Henry's law solubility (physical uptake). That is,

$$E = \frac{\int_0^t J(t')\,dt'}{2n_g HRT\sqrt{\frac{D_l t}{\pi}}} \tag{2}$$

In the bubble train, the measurements yield the numerator in eq 2. Mathematical solutions of the reacto−diffusive equations provide an expression for the enhancement factor (E) in terms of the reaction rate for specific cases.

For $Cl_2(g)$, the uptake is governed by the following processes:[23]

$$Cl_2(g) \rightleftarrows Cl_2(aq) \tag{R3}$$

$$Cl_2(aq) + H_2O \rightleftarrows HOCl + Cl^- + H^+ \tag{R1}$$

$$Cl_2(aq) + OH^- \rightleftarrows HOCl + Cl^- \tag{R2}$$

$$HOCl + OH^- \rightleftarrows OCl^- + H_2O \tag{R4}$$

(R1 and R2 are restated for convenience.) R1 and R2 are parallel processes followed by R4. Analytical expressions for the enhancement factor of the coupled R1, R2, and R4 reactions are not available. However, because these processes are effectively decoupled, gas uptake rates due to individual processes can be separated as a function of pH.

At low pH (pH ≈ 1, set with HCl), R2 and R4 are very slow, and R1 is nearly at equilibrium on the time scale of the present experiments ($t \leq 5$ s.). In this case, as demonstrated by Brian and co-workers[28,29] and Vivian and Peaceman,[30] $Cl_2(g)$ uptake is governed by physical solubility (R3) and can be quantitatively expressed via eq 1.

At intermediate pH (pH ≈ 7), the forward reactions R2 and R4 are slow because the near-surface OH^- is instantaneously depleted. The reverse reaction R1 is negligible, provided the concentrations of HOCl and Cl^- in the liquid are low. This is achieved by keeping the $Cl_2(g)$ concentration below 10^{18} cm^{-3}.[29] The $Cl_2(g)$ uptake is governed by the $Cl_2(aq)-H_2O$ forward reaction. The enhancement factor due to such an irreversible first-order reaction (with rate constant k_1) is[27]

$$E = (\pi k_1 t/4)^{1/2}[1 + 1/(2k_1 t)] \times \mathrm{erf}[(k_1 t)^{1/2}] + {}^1/_2\exp(-k_1 t) \tag{3}$$

With known values of H and D_l, the rate constant k_1 can be extracted from experimental data via eqs 1 and 3.

At high pH (pH > 9), the forward reaction R2 (with rate coefficient k_2), which is of principal interest in this study, dominates the uptake kinetics because the reverse reaction is negligible under our experimental conditions. Here, an approximation to the exact (numerical) solution for E, which was devised by Hikita and Asai,[31] can be applied:

$$E = [\gamma + \pi/8\gamma]\mathrm{erf}(2\gamma/\pi^{1/2}) + {}^1/_2\exp(-4\gamma^2/\pi) \tag{4}$$

where

$$\gamma = [\pi/4k_2[OH^-]t(E_i - E)/(E_i - 1)]^{1/2} \tag{5}$$

The parameter E_i is the "instantaneous enhancement factor". When this factor is much greater than 1, E_i can be expressed as[23,32]

$$E_i = (D_{Cl_2}/D_{OCl^-})^{1/2} + 0.8\{[OH^-]/[Cl_2(i)]\}(D_{OH^-}/D_{Cl_2})^{1/2} \tag{6}$$

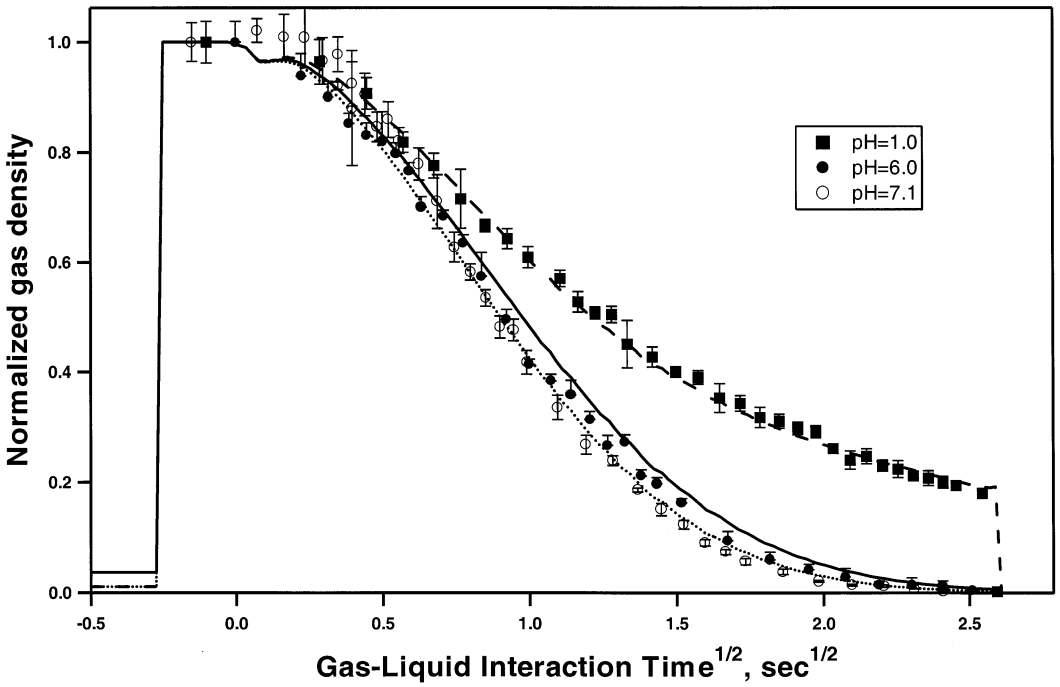

Figure 1. Normalized $Cl_2(g)$ density as a function of the square root of the gas−liquid interaction time. $T = 293$ K, and $Cl_2(g)$ number density = $(2-5) \times 10^{14}$ cm^{-3}. Lines are the best model fits to the data: (− − −) nonreactive uptake of $Cl_2(g)$ and (• • •) uptake governed by hydrolysis reaction R1.

where $Cl_2(i)$ is the interfacial concentration of chlorine in equilibrium with $Cl_2(g)$. (That is, at the interface, $Cl_2(i) = Cl_2(g)HRT$). The factor E_i takes into account the interfacial depletion of OH^- due to its reaction with $Cl_2(aq)$ and HOCl(aq) through R2 and R4, respectively.

A numerical model, which takes into account the specifics of the bubble train experiment (e.g., the changing size, shape, velocity, and convective mixing in the bubbles along their path), is used to relate the rate of trace gas disappearance to the fundamental physicochemical parameters (H, k, D) via the mathematical expressions provided above. The model also includes the effect of gas-phase diffusive transport on trace gas uptake. The details of the model are presented in Swartz et al.[24]

Experimental Results

The main purpose of this work is the measurement of the second-order rate constant of the $Cl_2(aq)/OH^-$ reaction. Therefore, the most detailed uptake studies were conducted in the high pH region, where this reaction dominates. The purpose of conducting studies at lower pH was mainly to connect our work to the relatively well-established results in the lower pH region.[19,28−30]

Uptake of $Cl_2(g)$ at Low pH. In Figure 1, we plot data (squares) for $Cl_2(g)$ uptake in 0.10 M hydrochloric acid at $T = 293$ K ($[Cl_2(g)] = 5 \times 10^{14}$ cm^{-3}). The y axis of the plot is the normalized density of the $Cl_2(g)$ remaining in the bubble after a gas−liquid interaction time t. (This is, in fact, the normalized mass spectrometer signal). As was discussed, chlorine uptake at low pH is governed by physical solubility (process R3), and the uptake is described by eq 1. As is evident from eq 1, it is convenient to plot $Cl_2(g)$ uptake as a function of $t^{1/2}$. The dashed line through the experimental points in Figure 1 is the best model fit of eq 1 to the uptake with the Henry's law coefficient as the variable parameter and the literature value[33] of $D_{Cl_2} = (1.48 \pm 0.08) \times 10^{-5}$ cm^{-2} s^{-1}. The optimization procedure yielded the value of $H_{Cl_2} = (6.5 \pm 0.5) \times 10^{-2}$ M atm^{-1} at 293 K.

Henry's law coefficients found in the literature[34] vary by about 40%, ranging from 6.2×10^{-2} to 9.8×10^{-2} M atm^{-1} at 298 K with a recommended value[35] of 9.29×10^{-2} M atm^{-1}. Our data is in reasonable agreement with the H values quoted in the literature. In our subsequent analysis, we will use our measured value of H at 293 K with the temperature dependence quoted by Whitney and Vivian,[36] that is, $H = 5.4 \times 10^{-2}\exp[3200(1/T - 1/T_0)]$ with $T_0 = 298$ K.

Uptake of $Cl_2(g)$ at Intermediate pH. In Figure 1, we also plot the data (circles) for chlorine uptake at pH = 6.0 and 7.1 ($[Cl_2(g)] = 2 \times 10^{14}$ cm^{-3}, $T = 293$ K). Because, as stated earlier, pH buffers were not used, $Cl_2(g)$ uptake leads to acidification of the near-surface liquid layer due to reactions R1, R2, and R4. The exact calculation of the time- and depth-resolved acidity of the liquid layer requires a solution for the differential equations describing simultaneous liquid-phase diffusion and chemical reactions R1−R4. However, an exact calculation of acidity is not necessary to identify the rate-controlling reaction. A simple calculation using the value of $k_1 = 15$ s^{-1} for the hydrolysis rate constant measured by Wang and Margerum[12] and values of k_2 for the $Cl_2(aq)/OH^-$ reaction measured in this work (see the next section) shows that the hydrolysis reaction dominates by at least a factor of 10 for pH < 5.5 ($[H^+] > 3 \times 10^{-6}$ M). At this pH, the initial H^+ concentration is negligible. The time required to reach this pH can be calculated from the following considerations. Essentially all $Cl_2(aq)$ is converted to H^+ via R1 and R2. (The reverse reactions are negligible.) Therefore, the time τ required to reach $[H^+] = [Cl_2(aq)] = 3 \times 10^{-6}$ M is obtained from

$$[(Cl_2(g) \text{ flux into the liquid})\tau]/\Delta x = 3 \times 10^{-6} \text{ M}$$

Here, Δx is the diffusion depth of $Cl_2(aq)$: $\Delta x = (D_{Cl_2}\tau)^{1/2}$. The $Cl_2(g)$ flux into the liquid is obtained from the experimental data. With the initial density of $[Cl_2(g)] = 2 \times 10^{14}$ cm^{-3} = 3.3×10^{-7} M and the bubble volume and surface area that were specified earlier, the $Cl_2(g)$ flux into the liquid (obtained from

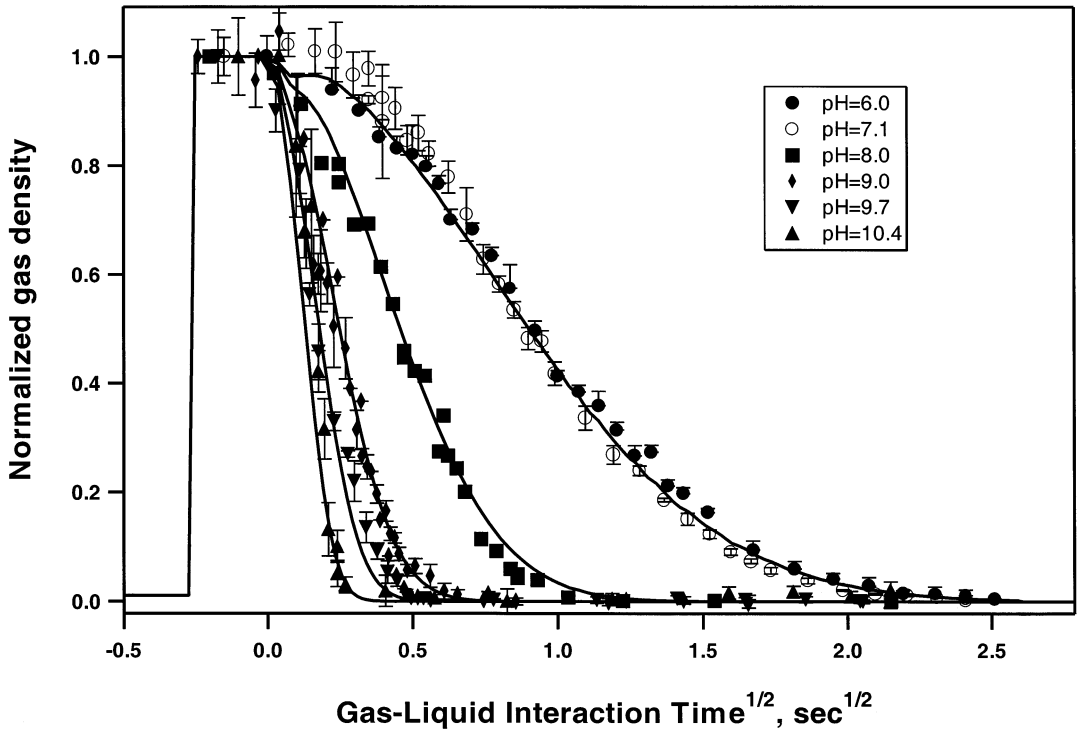

Figure 2. Normalized $Cl_2(g)$ density as a function of the square root of the gas−liquid interaction time in the higher pH region (pH = 6.0−11.0). $T = 293$ K, $Cl_2(g)$ number density $[Cl_2(g)] = 2 \times 10^{14}$ cm^{-3} for pH 6.0 and 7.1, and $[Cl_2(g)] = 5 \times 10^{13}$ cm^{-3} for pH = 8−11. Lines are the best model fits to the data.

the uptake data in Figure 1) is calculated to be 2×10^{13} cm^{-2} s^{-1}, with $D_{Cl_2} = 1.48 \times 10^{-5}$ cm^2 s^{-1}, $\tau \approx 0.15$ s. This is a negligible fraction of the experimental uptake time of about 5 s. Therefore, with the initial pH set at 6.0 or 7.1, the $Cl_2(g)$ uptake is governed by the hydrolysis reaction R1.

The solid line in Figure 1 is the model fit to the uptake data (eq 3) governed by the hydrolysis reaction R1 with $k_1 = 15$ s^{-1}, as determined by Wang and Margerum in a flow tube experiment.[12] The best fit to our data is shown as a dotted line, which yields a value of $k_1 = (22 \pm 4)$ s^{-1} at 293 K.

These experiments were also performed at 275 and 303 K with $Cl_2(g)$ densities ranging from 1×10^{14} to 5×10^{14} cm^{-3}. A similar fitting procedure yielded best-fit values for the $Cl_2(aq)$ hydrolysis rate constant: $k_1 = (4.5 \pm 1)$ s^{-1} at 275 K and (34 ± 8) s^{-1} at 303 K. These results are within about 40% of the median k_1 values measured by Wang and Margerum[12] and within about 14% of the lower limit of their measurement.

Uptake of $Cl_2(g)$ at High pH. In Figure 2, we plot a set of $Cl_2(g)$ uptake data at high pH (pH = 8−11). As is evident, the uptake rate increases with pH. The rate-controlling process here is the $Cl_2(aq) + OH^-$ reaction (R2). The interfacial concentration of OH^- is depleted via reactions R1, R2, and R4. The formulation of eqs 4−6 takes into account this depletion (as is stated in the Modeling Chlorine Uptake section). The validity of the overall treatment of the OH^- depletion (when significant) is confirmed by the fact that the derived values of k_2 are independent of initial OH^- concentration over a range of 3 orders of magnitude. Furthermore, the measured value of k_2 remains constant when the $Cl_2(g)$ density at pH = 9.7 is varied from 6×10^{13} to 2×10^{15} cm^{-3}.

Solid lines in Figure 2 are best model fits to the experimental data, with k_2 as a variable parameter. The following values were used for the liquid-phase diffusion coefficients at $T = 298$ K: $D_{OH^-} = (5.3 \pm 0.1) \times 10^{-5}$ cm^{-2} s^{-1} (MacInnes[37]), and $D_{OCl^-} = (1.2 \pm 0.2) \times 10^{-5}$ cm^{-2} s^{-1} (Hikita et al.[23]). The Stokes−Einstein relationship was used to obtain diffusion coefficients at the other temperatures.

The experiments were performed at 275, 293, and 303 K. In Figure 3, we plot the measured second-order rate constant (k_2) for the $Cl_2(aq)/OH^-$ reaction as a function of OH^- concentration at the three temperatures. The dashed lines are the average values of k_2 measurements: $(1.3 \pm 0.5) \times 10^8$ M^{-1} s^{-1} at 275 K, $(6 \pm 2) \times 10^8$ M^{-1} s^{-1} at 293 K, and $(8 \pm 3) \times 10^8$ M^{-1} s^{-1} at 303 K.

The main source of uncertainty in the quoted k_2 values is the tightness of the model fit to the measured gas uptake with respect to k_2. The 30−40% error limits represent the statistical uncertainty (one standard deviation) in the model fit to the uptake data points.

The uncertainties in the diffusion coefficients D_{OH^-}, D_{OCl^-}, and D_{Cl_2} used in our calculations are not expected to degrade the accuracy of the k_2 determinations. The diffusion coefficients of the two ionic species appear in the form of D_{OH^-}/D_{OCl^-} (see eq 6). The value of D_{OH^-} that is calculated from ionic conductivities using the Nernst formula is well established (to within 2%).[37] The ionic conductance of OCl^- has not been measured but was obtained via extrapolation by Hikita et al.[23] The estimated accuracy of the conductivity extrapolation and, therefore, of the diffusion coefficient is estimated to be ±20%. The numerical model for the calculation of k_2 is not highly sensitive to the diffusion coefficients of the ions. For example, a 20% change in D_{OCl^-} produces only a 6% change in k_2, which is well within the accuracy of our experimental measurements. The value of k_2 depends linearly (at most) on D_{Cl_2}. This parameter, however, is well established, with a reproducibility of about 5%.[33]

The gas-phase diffusion correction is included in the numerical model as discussed in ref 24. In the present experiments, this correction is significant (about 30%) only for the fastest $Cl_2(g)$ uptake at pH = 11.

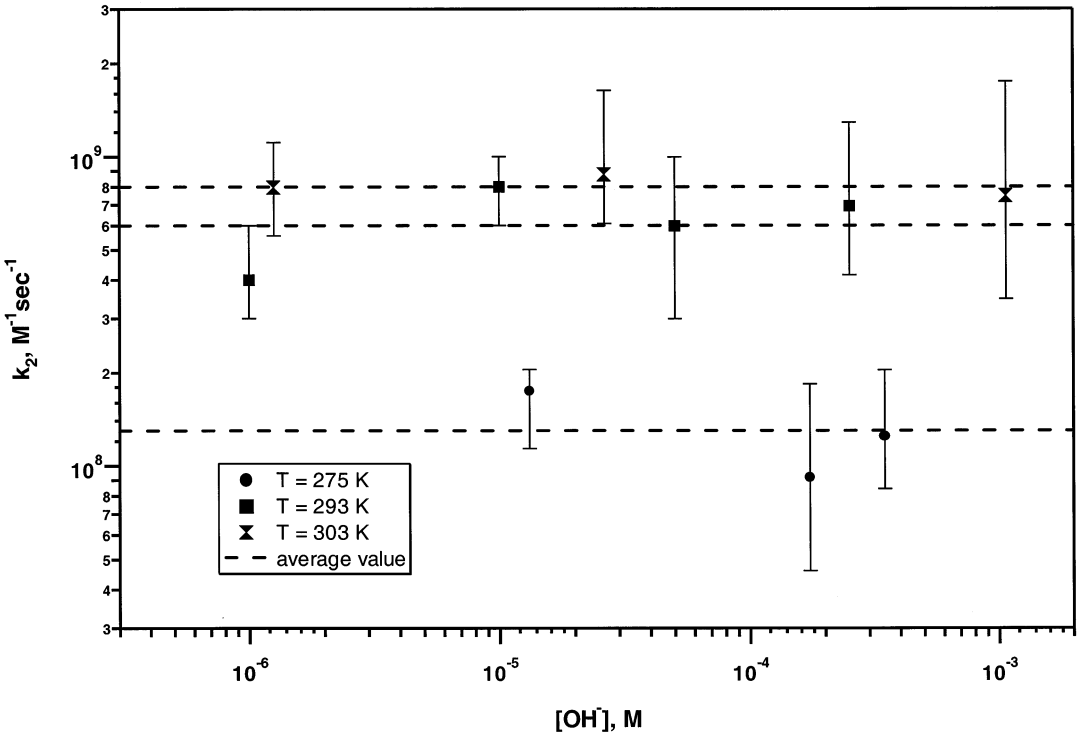

Figure 3. Second-order rate constant k_2 for the Cl_2/OH^- reaction as a function of $[OH^-]$ at $T = 275$, 293, and 303 K. Dashed lines are the average values for k_2 measurements.

Finally, we note that in extracting k_2 values from the uptake measurements the effect of mass accommodation (interfacial mass transport) has been assumed not to affect $Cl_2(g)$ uptake. Whereas the magnitude of the mass accommodation coefficient of $Cl_2(g)$ on water is not known, we conclude that it does not hinder $Cl_2(g)$ uptake because even the fastest uptake is well characterized by a purely reactive uptake, as expressed by eqs 4−6.

Discussion

Because the values in the Table 1 are considered to be estimates by the authors, comparison with our k_2 measurements may not be meaningful, even for the two values that are within about a factor of 2 of our measurements. For example, the agreement with the data of Lifshitz and Perlmutter-Hayman[17] is likely fortuitous because, as stated earlier, their k_2 value is obtained from a long-range extrapolation. However, the agreement with the k_2 values of Ashour et al.[20] is likely more than a coincidence. Their k_2 values were obtained from direct measurements utilizing numerical integration of mass transfer equations for data analysis. The agreement of their k_2 values with ours likely indicates that their method of data analysis properly took into account the effect of high $Cl_2(g)$ densities used in their experiments.

Atmospheric Implications

With a known value of k_1 for reaction R1, the present determination of k_2 for R2 allows one to compare the effects of processes R1 and R2 on the depletion of $Cl_2(aq)$ in aerosols. The relative importance of R1 and R2 is, of course, pH-dependent. At atmospheric densities of $Cl_2(g)$ ($\sim 10^3-10^4$ cm^{-3}), acidification of aerosol due to $Cl_2(g)$ uptake is negligible. The pH value at which the forward rates R1 and R2 are equal is obtained from $k_1 = k_2[OH^-]$, yielding pH = 6.6. Above this pH, R2 dominates. The pH of fresh aerosols and seawater is often close to 6,[38] whereas older aerosols are usually more acidic.[39−41] However, for typical aerosol sizes, both of these chemical pathways are slow compared to the rate of $Cl_2(aq)$ diffusion to the surface and evaporation out of the particle. For example, in a 1-μm particle at pH = 7, the characteristic time of diffusion is about 100 times faster than the characteristic time of reactions R1 and R2. In that case, only at pH ≥ 9 does R2 compete with diffusion-limited $Cl_2(aq)$ evaporation.

Acknowledgment. We thank Mr. E. M. Knipping, Professor D. Dabdub, and Professor B. J. Finlayson-Pitts for their encouragement and helpful discussions. Funding for this work was provided by the National Science Foundation Grant Nos. ATM-99-05551 and CH-0089147, the Department of Energy Grant No. DE-FG02-98ER62581, and the US−Israel Binational Science Foundation Grant No. 1999134.

References and Notes

(1) Rudolph, J.; Koppmann, R.; Plass-Dulmer, Ch. *Atmos. Environ.* **1996**, *30*, 1887−1894.

(2) Singh, H. B.; Thakur, A. N.; Chen, Y. E.; Kanakidou, M. *Geophys. Res. Lett.* **1996**, *23*, 1529−1532.

(3) Spicer, C. W.; Chapman, E. G.; Finlayson-Pitts, B. J.; Plastridge, R. A.; Hubbe, J. M.; Fast, J. D.; Berkowitz, C. M. *Nature (London)* **1998**, *394*, 353−356.

(4) Keene, W. C.; Pszenny, A. A. P.; Jacob, D. J.; Duce, R. A.; Galloway, J. N.; Schultz-Tokos, J. J.; Sievering, H.; Boatman, J. F. *Global Biogeochem. Cycles* **1990**, *4*, 407−30.

(5) Wingenter, O. W.; Kubo, M. K.; Blake, N. J.; Smith, T. W., Jr.; Blake, D. R.; Rowland, F. S. *J. Geophys. Res., [Atmos.]* **1996**, *101*, 4331−4340.

(6) Singh, H. B.; Gregory, G. L.; Anderson, B.; Browell, E.; Sachse, G. W.; Davis, D. D.; Crawford, J.; Bradshaw, J. D.; Talbot, R.; et al. *J. Geophys. Res., [Atmos.]* **1996**, *101*, 1907−1917.

(7) Caloz, F.; Fenter, F. F.; Rossi, M. J. *J. Phys. Chem.* **1996**, *100*, 7494−7501.

(8) Gebel, M. E.; Finlayson-Pitts, B. J. *J. Phys. Chem. A* **2001**, *105*, 5178−5187.

(9) Gershenzon, M. Y.; Il'in, S.; Fedotov, N. G.; Gershenzon, Y. M.; Aparina, E. V.; Zelenov, V. V. *J. Atmos. Chem.* **1999**, *34*, 119−135.

(10) Knipping, E. M.; Lakin, M. J.; Foster, K. L.; Jungwirth, P.; Tobias, D. J.; Gerber, R. B.; Dabdub, D.; Finlayson-Pitts, B. J. *Science (Washington, D.C.)* **2000**, *288*, 301−306.

(11) Knipping, E. M.; Dabdub. D. *J. Geophys. Res.*, submitted for publication, 2001.

(12) Wang, T. X.; Margerum, D. W. *Inorg. Chem.* **1994**, *33*, 1050−1055.

(13) Shilov, E. A.; Solodushenkov, S. M. *Compt. Rend. Acad. Sci. URSS* **1936**, *1*, 96.

(14) Shilov, E. A.; Solodushenkov, S. M. *J. Phys. Chem. (U.S.S.R.)* **1945**, *19*, 404.

(15) Morris, J. C. *J. Am. Chem. Soc.* **1946**, *68*, 1692−1694.

(16) Anbar, M.; Taube, H. *J. Am. Chem. Soc.* **1958**, *80*, 1073−1077.

(17) Lifshitz, A.; Perlmutter-Hayman, B. *J. Phys. Chem.* **1962**, *66*, 701−705.

(18) Eigen, E.; Kustin, K. *J. Am. Chem. Soc.* **1962**, *84*, 1355−1361.

(19) Spalding, C. W. *AIChE J.* **1962**, *8*, 685−689.

(20) Ashour, S. S.; Rinker, E. B.; Sandall, O. C. *AIChE J.* **1996**, *42*, 671−682.

(21) Sandall, O. C.; Goldberg, I. B.; Hurlock, S. C.; Laeger, H. O.; Wagner, R. I. *AIChE J.* **1981**, *27*, 856−859.

(22) Takahashi, T.; Hatanaka, M.; Konaka, R. *Can. J. Chem. Eng.* **1967**, *45*, 145−149.

(23) Hikita, H.; Asai, S.; Himukashi, Y.; Takatsuka, T. *Chem. Eng. J. (Lausanne)* **1973**, *5*, 77−84.

(24) Swartz, E.; Boniface, J.; Tchertkov, I.; Rattigan, O. V.; Robinson, D. V.; Davidovits, P.; Worsnop, D. R.; Jayne, J. T.; Kolb, C. E. *Environ. Sci. Technol.* **1997**, *31*, 2634−2641.

(25) Cheung, J. L.; Li, Y. Q.; Boniface, J.; Shi, Q.; Davidovits, P.; Worsnop, D. R.; Jayne, J. T.; Kolb, C. E. *J. Phys. Chem. A* **2000**, *104*, 2655−2662.

(26) Gershenzon, M.; Davidovits, P.; Jayne, J. T.; Kolb, C. E.; Worsnop, D. R. *J. Phys. Chem.* **2001**, *105*, 7031−7036.

(27) Danckwerts, P. V. *Gas−Liquid Reactions;* Chemical Engineering Series; McGraw-Hill: New York, 1970.

(28) Gilliland, E. R.; Baddour, R. F.; Brian, P. L. T. *AIChE J.* **1958**, *4*, 223−230.

(29) Brian, P. L. T.; Vivian, J. E.; Habib, A. G. *AIChE J.* **1962**, *8*, 205−209.

(30) Vivian, J. E.; Peaceman, D. W. *AIChE J.* **1956**, *2*, 437−443.

(31) Hikita, H. A.; Asai, S. *Int. Chem. Eng.* **1964**, *4*, 332−340.

(32) Hikita, H.; Asai, S.; Takatsuka, T. *Chem. Eng. J. (London)* **1972**, *4*, 31−40.

(33) Himmelblau, D. M. *Chem. Rev.* **1964**, *64*, 527.

(34) Sander, R. *Henry's Law Constants*; In NIST Chemistry Webbook, National Institute of Standards and Technology, Database Number 69, Gaithersburg, MD 20899. http://webbook.nist.gov (accessed July 2001).

(35) Huie, R. E. National Institute of Standards and Technology. Private communication, 2001.

(36) Whitney, R. P.; Vivian, J. E. *Ind. Eng. Chem.* **1941**, *33*, 741.

(37) MacInnes, D. *The Principles of Electrochemistry;* Dover Publications: New York, 1961.

(38) Keene, W. C.; Sander, R.; Pszenny, A. A. P.; Vogt, R.; Crutzen, P. J.; Galloway, J. N. *J. Aerosol Sci.* **1998**, *29*, 339−356.

(39) Keene, W. C.; Savoie, D. L. *Geophys. Res. Lett.* **1998**, *25*, 2181−2184.

(40) Keene, W. C.; Savoie, D. L. *Geophys. Res. Lett.* **1999**, *26*, 1315.

(41) Von Glasow, R.; Sander, R. *Geophys. Res. Lett.* **2001**, *28*, 247−250.